On the cause of eastern equatorial Pacific Ocean T-S variations associated with El Niño

Ou Wang, Ichiro Fukumori, Tong Lee, and Benny Cheng
Jet Propulsion Laboratory, California Institute of Technology, Pasadena, California, USA

Received 6 April 2004; accepted 9 July 2004; published 12 August 2004.

[1] The nature of observed variations in temperature-salinity (T-S) relationship between El Niño and non-El Niño years in the pycnocline of the eastern equatorial Pacific Ocean (NINO3 region, 5°S–5°N, 150°W–90°W) is investigated using an ocean general circulation model. The origin of the subject water mass is identified using the adjoint of a simulated passive tracer. The higher salinity during El Niño is attributed to larger convergence of saltier water from the Southern Hemisphere and smaller convergence of fresher water from the Northern Hemisphere. *INDEX TERMS:* 4215 Oceanography: General: Climate and interannual variability (3309); 4522 Oceanography: Physical: El Niño; 4536 Oceanography: Physical: Hydrography; 4231 Oceanography: General: Equatorial oceanography; 4255 Oceanography: General: Numerical modeling. **Citation:** Wang, O., I. Fukumori, T. Lee, and B. Cheng (2004), On the cause of eastern equatorial Pacific Ocean T-S variations associated with El Niño, *Geophys. Res. Lett.*, *31*, L15309, doi:10.1029/2004GL020188.

1. Introduction

[2] Interannual variations in temperature-salinity (T-S) relationship are found in the eastern equatorial Pacific associated with El Niño; water tends to become saltier (and therefore warmer) during El Niño years on density surfaces within the pycnocline [*Mangum et al.*, 1986; *Johnson et al.*, 2002; *Wang et al.*, 2004]. A numerical model used in the latter study successfully simulates the observed T-S change and further suggests a large-scale coherent change in circulation associated with this variability.

[3] Understanding this shift in T-S relationship is important as it may alter the near-surface circulation, which in turn changes the sea surface temperature to affect air-sea interaction. Air-sea interaction is crucial to adjustments associated with El Niño/Southern Oscillation (ENSO) by changing winds and heat fluxes [e.g., *Zebiak and Cane*, 1987]. Understanding changes in T-S relationships is also important for some data assimilation schemes that otherwise assume time-invariant T-S relationships [*Troccoli and Haines*, 1999; *Maes et al.*, 2002]. It is not obvious why there is saltier water in the eastern equatorial Pacific Ocean during El Niño events. Upwelling and strong stratification in the upper eastern equatorial Pacific Ocean make it difficult for changes in evaporation-precipitation during El Niño to reach the lower pycnocline [*Johnson et al.*, 2000]. Change in advection is a more likely cause for the T-S variations associated with El Niño.

0094-8276/04/2004GL020188$05.00

[4] The objective of this paper is to investigate the nature and cause of the T-S variations in the pycnocline of the eastern equatorial Pacific Ocean associated with El Niño events. To this end, the change in ocean circulation underlying the T-S variations is investigated using an ocean general circulation model. Specifically, the adjoint of a simulated passive tracer is used to trace backwards in time the origin of the water following the method used by *Fukumori et al.* [2004]. The "origin" herein refers to where the water mass comes from on interannual time scales, not the ultimate source where it initially obtains its T-S characteristics through atmospheric forcing.

2. Numerical Model and Adjoint Passive Tracer

[5] We use the same ocean circulation model as *Wang et al.* [2004] to analyze the cause of the observed T-S variations. The model is based on the Massachusetts Institute of Technology General Circulation Model (MITgcm). The model is run with a near-global domain (79.5°S–78.5°N), forced by National Centers for Environmental Prediction reanalysis products (12-hourly wind stress, daily diabatic air-sea fluxes) with time-means replaced by those of the Comprehensive Ocean-Atmosphere Data Set (see *Marshall et al.* [1997a, 1997b] and *Lee et al.* [2002] for detailed model description and setup). Model resolution is 1° horizontally except within 10° of the Equator where meridional resolution gradually decreases to 0.3°, and 10-m vertically in the upper 150 m with total 46 vertical levels (deepest sea bottom is set to 5815-m). The *Gent and McWilliams* [1990] isopycnal mixing scheme and the KPP mixed-layer formulation [*Large et al.*, 1994] are employed. After a 10-year spin-up starting from rest using climatological temperature and salinity distributions [*Boyer and Levitus*, 1997], the simulation is run from 1980 to present. The general circulation and water properties by the numerical simulation are reasonably consistent with observational data [*Lee et al.*, 2002; *Lee and Fukumori*, 2003; *Wang et al.*, 2004].

[6] The adjoint of the simulated passive tracer integrated backwards in time can be viewed as describing where a tracer-tagged water comes from. In continuous form, the adjoint passive tracer equation is identical to the forward passive tracer equation, except for the reversal of signs of all terms but diffusion

$$-\frac{\partial c}{\partial t} = \mathbf{u} \cdot \nabla c + \nabla \cdot \kappa \nabla c, \tag{1}$$

where c is the tracer concentration, $\mathbf{u}$ is the velocity vector, and κ is the mixing tensor. Both $\mathbf{u}$ and κ are obtained from a forward integration of the model. Thus c evolves

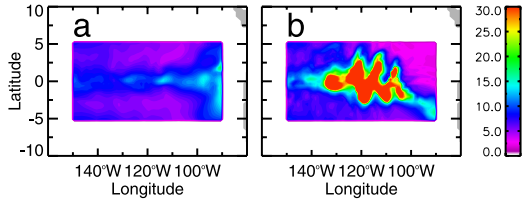

Figure 1. Vertical integral of adjoint tracer (in arbitrary tracer units per area, ATU m^{-2}) occupying the pycnocline layer $24.5 \leq \sigma_\theta \leq 25$ kg m^{-3} of the NINO3 region at the terminal instant (a) at the end of 1997 and (b) at the end of 1996.

identically with the water mass within the model backwards in time.

[7] Given a terminal adjoint tracer distribution that is uniform over a particular volume and zero elsewhere with no sources or sinks, adjoint tracer values evaluated by (1) at earlier instances can be interpreted as describing the fraction of the water that would converge to the terminal tracer-tagged volume. For instance, if the terminal value were 1 in an arbitrary tracer unit, a value of 0.3 somewhere at an earlier instant implies that 30% of this water mass would reach the terminal tracer-tagged volume. Given the conservative nature of (1), the global integral of the adjoint tracer is time-invariant. That is, the distribution of adjoint tracer describes where all the water in the terminal volume originates at earlier instances. See *Fukumori et al.* [2004] for further discussion and model implementation of using passive tracers and their adjoint to deduce pathways of water masses.

[8] As was done by *Wang et al.* [2004], we focus on the water in the pycnocline layer of NINO3 (5°S–5°N, 150°W–90°W). The origin of this water mass is examined by integrating the adjoint tracer equation backwards in time releasing adjoint tracers in the subject volume at the terminal instant. The origins of waters occupying the NINO3 region at the end of 1997 (an El Niño year) and that of 1996 (a non-El Niño year) are examined separately. Integrations are carried out for one year. A one year integration is sufficient, as described below, to distinguish differences in the origin of the water of these two instances.

3. Results

3.1. Tracer Distribution

[9] The terminal adjoint passive tracer is set to a unit concentration (in arbitrary tracer units per volume, ATU m^{-3}) in the NINO3 pycnocline layer $24.5 \leq \sigma_\theta \leq 25$ kg m^{-3} (σ_θ is potential density anomaly), where the maximum T-S variations were observed [*Wang et al.*, 2004]. Figure 1a is the vertical integral (from the sea surface to the bottom) of tracer concentration at the terminal instant of end of Year 1997. The inhomogeneities within NINO3 reflects spatial variations in the thickness of the thermocline. The tracer distribution is approximately symmetric along the Equator, with relatively large values along the Equator and in the eastern equatorial Pacific Ocean and small concentration in the north and south regions off the Equator. In contrast, the tracer distribution at the end of Year 1996 is less symmetric, with large concentration along or near the Equator, and small concentration in the northeastern part of the NINO3 region (Figure 1b). The total amount of tracer at the end of 1997 is 56% of that at the end of 1996, reflecting an overall thinner pycnocline for the former time instant.

[10] Figures 2a–2d show the backward time evolution of the vertical integral of adjoint tracer, at three-month intervals from the terminal instant of December 1997. The tracer concentration has been normalized by the total amount of terminal tracer concentration. The tracer cloud separates backwards in time, and by June 1997 (six months prior to the terminal instant) three patches of tracer are well identifiable. In January 1996 (one year prior to the terminal instant), most water of the pycnocline layer of the NINO3 region can be seen to originate from (1) the western equatorial Pacific warm pool, (2) south of the Equator with maximum concentration centered near 8°S, 125°W, and (3) north of the Equator between 170°E and 120°W with maximum concentration along 6°N. There is only a small tracer concentration east of 110°W, likely due to the reduced strength or even reversal of the South Equatorial Current in the eastern Pacific Ocean during El Niño events.

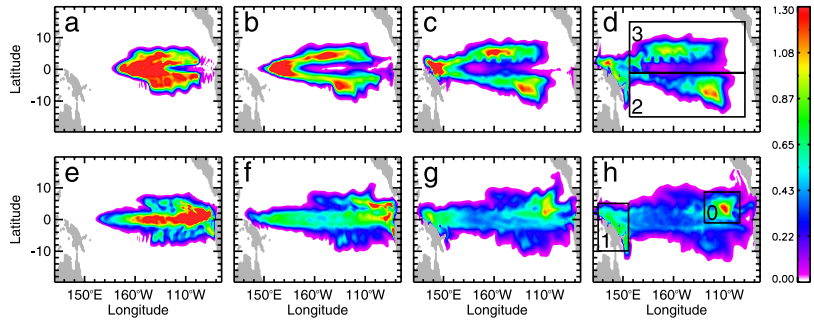

Figure 2. Evolution of vertical integral of adjoint tracer, at (a) −3, (b) −6, (c) −9, (d) −12 months from the terminal instant at the end of Year 1997. The lower panels show (e) −3, (f) −6, (g) −9, (h) −12 months from the terminal instant at the end of Year 1996. The values have been normalized by the total amount of corresponding terminal tracer concentration (units in 10^{-13} m^{-2}), so that a global area integral of the values is one. The outlined boxes correspond to areas of time series of salt contribution shown in Figure 5. The boxes are defined as: Box 0, 1°S–8.7°N, 130°W–95°W; Box 1, 10°S–5°N, 125°E–155°E; Box 2, 15°S–1°S, 156°E–90°W; Box 3, 1°S–15°N, 156°E–90°W.

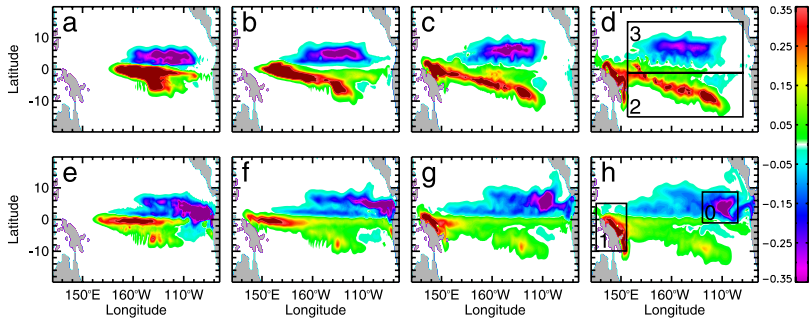

Figure 3. Evolution of vertical integral of adjoint tracer-weighted salinity anomaly at (a) −3, (b) −6, (c) −9, (d) −12 months from the terminal instant at the end of Year 1997. The lower panels show (e) −3, (f) −6, (g) −9, (h) −12 months from the terminal instant at the end of Year 1996. The values have been normalized by the total amount of corresponding terminal tracer concentration (units in 10^{-13} psu m^{-2}). The outlined boxes are the same as those defined in Figure 2, and correspond to areas of time series of salt contribution shown in Figure 5.

[11] The results from Year 1996, a non-El Niño year, are very different from those for Year 1997 (Figures 2e–2h). Apart from water from the western equatorial Pacific warm pool and from south and north of the Equator, a significant amount of the NINO3 water is found originating in the east. In June 1996 (six months prior to the terminal instant), the water from the east is mainly from the region east of 110°W centered along 2.5°N. One year prior to the terminal instant in December 1996, most tracers from the east are from the region south of the Costa Rica Dome region. In fact, a significant amount of NINO3 *surface* water also originates from the same region for a non-El Niño year [*Fukumori et al.*, 2004].

[12] Vertically, the pathways generally remain within the pycnocline $22 \leq \sigma_\theta \leq 26$ kg m^{-3} (not shown). The exceptions are the pathway south of the Costa Rica Dome region that is mainly near the surface, and that near the Equator east of the date line where part of the water is found to originate from depths below $\sigma_\theta = 26$ kg m^{-3}.

[13] In spite of large-scale differences, comparable amounts of water (7%) originate from the western equatorial Pacific warm pool for both 1996 and 1997 NINO3 water (Box 1, see boxes in Figure 2). Significant differences are found in the Northern and Southern Hemispheres and in the eastern domain. Less water (54%) is of Northern Hemisphere origin (>1°S of latitude, Box 3) for 1997 water than it is for 1996 water (61%). In contrast, more water (39%) is of Southern Hemisphere origin (≤1°S, Box 2) for 1997 water than it is for 1996 water (28%). Less water (15%) is from the eastern Pacific Ocean (Box 0) for 1997 water than it is for 1996 water (32%). Difference in relative T-S contributions that arises from these variations are further investigated below.

3.2. Salt Contribution

[14] The adjoint tracer discussed in subsection tracer distribution only described where the tracer-tagged water came from. The adjoint tracer, when weighted by coincident salinity (i.e., salinity at the same time and location), provides a means to evaluate the salt contribution by the source waters. Figure 3 shows the backward time evolution of vertical integral of adjoint tracer-weighted salinity anomaly $c(s - s_0)$. c is the adjoint tracer normalized by the total amount of released terminal tracer. s_0 is mean salinity averaged on isopycnals of the NINO3 region for the two year period (1996–1997). Positive values indicate that the water from that region at a given instant increases the salinity of the NINO3 pycnocline water at the terminal instant, while negative values indicate otherwise. For water of Year 1997, water from the western equatorial Pacific warm pool and from the Southern Hemisphere increases the salinity of the NINO3 pycnocline water (positive contribution), while water from the north decreases the salinity of NINO3 water (negative contribution, Figures 3a–3d).

[15] For Year 1996 water, positive salt contribution is from the west and the south (Figures 3e–3h). As in Year 1997, contribution from the north is negative, but the most distinguishable is from the eastern Pacific east of 120°W. At one year prior to the end of Year 1996, the maximum negative salt contribution is from the region south of the Costa Rica Dome region.

[16] The salinity distribution is asymmetric about the Equator. On a given isopycnal surface in the thermocline the water south of the Equator and that from the western equatorial Pacific warm pool are saltier than water from the north [e.g., *Johnson and McPhaden*, 1999; *Kessler*, 1999]. Figure 4 shows the model's salinity distribution on $\sigma_\theta = 25$ kg m^{-3} in January 1997 (Figure 4a) and January 1996 (Figure 4b). The distribution at other instances are similar and are thus not shown. Saltier waters from the western equatorial Pacific warm pool and from the Southern Hemisphere increase the salinity of the NINO3 pycnocline water, as shown by the positive contribution in Figure 3, while fresher water from the Northern Hemisphere has a negative contribution.

[17] To quantify the salt contribution of different regions, the total tracer weighted salinity anomaly is evaluated over

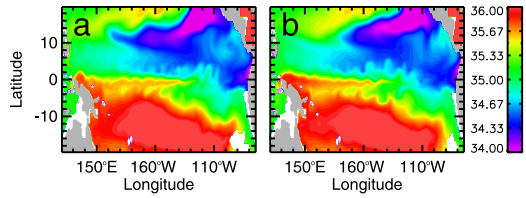

Figure 4. Salinity (psu) on density surface $\sigma_\theta = 25$ kg m^{-3} at (a) January 1997 (12 months prior to the terminal instant of Year 1997) and (b) January 1996 (12 months prior to the terminal instant of Year 1996).

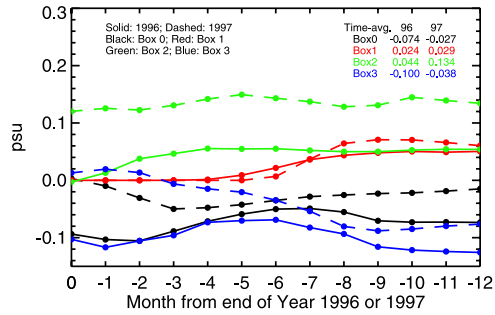

Figure 5. The salt contribution, defined as the volume integral of adjoint tracer-weighted salinity anomaly, to the NINO3 water from the region south of the Costa Rica Dome region (Box 0 in Figure 3, black), the western equatorial Pacific warm pool (Box 1, red), the Southern Hemisphere (Box 2, green), and the Northern Hemisphere (Box 3, blue). Solid and dashed curves correspond to terminal Years 1996 and 1997, respectively. The values have been normalized by the total amount of corresponding terminal tracer concentration (units in psu).

four regions (Boxes 0–3 as defined in Figure 2; the same boxes also shown in Figure 3) and is shown as time-series in Figure 5. Salt contributions from the western equatorial Pacific warm pool (Box 1 in Figure 3) are comparable for Years 1996 and 1997 (red curves in Figure 5, solid for 1996 water). The salt contribution from the Northern Hemisphere (Box 3) for Year 1996 water is negative with the magnitude larger than that for Year 1997 water (blue curves). The difference of salt contribution for the two years in the Northern Hemisphere is primarily the difference in Box 0, a sub-region of Box 3. Positive contribution from the Southern Hemisphere (Box 2) for 1997 water is much larger than that for 1996 water (green curves), due to a larger amount of water originating there in 1997. It is this large positive contribution of salt as well as the small magnitude of negative contribution from the Northern Hemisphere that increases the salinity of the NINO3 pycnocline water in 1997.

[18] Differences in salt contribution discussed above, especially at 12 months prior to the terminal instant, are due to different origins of the water masses (i.e., distribution of adjoint tracer) as opposed to differences in hydrography (i.e., salinity distribution). For instance, the difference in salinity distribution between January 1996 and January 1997 is sufficiently small that $c(s - s_0)$ using s at January 1997 is nearly the same as for s at January 1996 (not shown).

4. Conclusion

[19] Interannual T-S relationship variations in the eastern equatorial Pacific have been found during the period of 1980 to 1999. In situ CTD observations and a numerical simulation suggest that water in the NINO3 region tends to become saltier (and therefore warmer) during El Niño events on isopycnals within the pycnocline, especially for water of $24.5 \leq \sigma_\theta \leq 26$ kg m^{-3} [*Wang et al.*, 2004]. This study investigates the nature and cause of the interannual T-S relationship variations between the period of 1996 and 1997 using the adjoint of a simulated passive tracer. Origins of the NINO3 pycnocline water are found to be substantially different for 1996 and 1997.

[20] One year prior to the end of 1997, an El Niño year, water is mainly from (1) the western equatorial Pacific warm pool, (2) north of the Equator centered at 6°N, 170°W, and (3) south of the Equator centered at 8°S, 125°W, while one year prior to the end of 1996 the water is mainly from (1) the western equatorial Pacific warm pool and (2) north of the Equator centered at 4°N, 110°W. Less water is of northern origin and more water is of southern origin for 1997 water than it is for 1996 water. Because of the north-south asymmetry in salinity on a given isopycnal [*Johnson and McPhaden*, 1999; *Kessler*, 1999], the additional water of southern origin and less water of northern origin give rise to the observed T-S anomaly in the NINO3 region during El Niño.

[21] Similar circulation differences are found for T-S anomalies simulated by *Wang et al.* [2004] associated with other El Niño/non-El Niño years. In particular, from 1980 to 1999, the amount of NINO3 water originating in the northern and southern hemispheres averaged over the one-year period prior to reaching NINO3 is correlated with the Southern Oscillation Index at the 95% confidence level.

[22] **Acknowledgments.** This work was carried out at the Jet Propulsion Laboratory, California Institute of Technology, under a contract with the National Aeronautics and Space Administration (NASA). This study is a contribution of the Consortium for Estimating the Circulation and Climate of the Ocean (ECCO) funded by the National Oceanographic Partnership Program.

References

Boyer, T. P., and S. Levitus (1997), Objective analysis of temperature and salinity for the world Ocean on a 1/4° grid, *NOAA Atlas NESDIS*, vol. 11, 62 pp., Dep. of Comm., Washington, D. C.

Fukumori, I., T. Lee, B. Cheng, and D. Menemenlis (2004), The origin, pathway, and destination of Niño-3 water estimated by a simulated passive tracer and its adjoint, *J. Phys. Oceanogr.*, *34*, 582–604.

Gent, P., and J. McWilliams (1990), Isopycnal mixing in ocean circulation models, *J. Phys. Oceanogr.*, *20*, 150–155.

Johnson, G. C., and M. J. McPhaden (1999), Interior pycnocline flow from the subtropical to the equatorial Pacific Ocean, *J. Phys. Oceanogr.*, *29*, 3073–3089.

Johnson, G. C., M. J. McPhaden, G. D. Rowe, and K. E. McTaggart (2000), Upper equatorial Pacific Ocean current and salinity variability during the 1996–1998 El Niño–La Niña cycle, *J. Geophys. Res.*, *105*, 1037–1053.

Johnson, G. C., B. M. Sloyan, W. S. Kessler, and K. E. McTaggart (2002), Direct measurements of upper ocean currents and water properties across the tropical Pacific Ocean during the 1990s, *Prog. Oceanogr.*, *52*, 31–61.

Kessler, W. S. (1999), Interannual variability of the subsurface high salinity tongue south of the equator at 165°E, *J. Phys. Oceanogr.*, *29*, 2038–2049.

Large, W. G., J. C. McWilliams, and S. C. Doney (1994), Oceanic vertical mixing: A review and a model with a nonlocal boundary layer parameterization, *Rev. Geophys.*, *32*, 363–403.

Lee, T., and I. Fukumori (2003), Interannual-to-Decadal variations of tropical-subtropical exchange in the Pacific Ocean: Boundary versus interior pycnocline transports, *J. Clim.*, *16*, 4022–4042.

Lee, T., I. Fukumori, D. Menemenlis, Z. Xing, and L.-L. Fu (2002), Effects of the Indonesian Throughflow on the Pacific and Indian Oceans, *J. Phys. Oceanogr.*, *32*, 1404–1429.

Maes, C., M. J. McPhaden, and D. Behringer (2002), Signatures of salinity variability in tropical Pacific Ocean dynamic height anomalies, *J. Geophys. Res.*, *107*(C12), 8012, doi:10.1029/2000JC000737.

Mangum, L. J., S. P. Hayes, and J. M. Toole (1986), Eastern Pacific Ocean circulation near the onset of the 1982–1983 El Niño, *J. Geophys. Res.*, *91*, 8428–8436.

Marshall, J., A. Adcroft, C. Hill, L. Perelman, and C. Heisey (1997a), A finite-volume, incompressible Navier-Stokes model for studies of the ocean on parallel computers, *J. Geophys. Res.*, *102*, 5753–5766.

Marshall, J., C. Hill, L. Perelman, and A. Adcroft (1997b), Hydrostatic, quasi-hydrostatic and non-hydrostatic ocean modeling, *J. Geophys. Res.*, *102*, 5733–5752.

Troccoli, A., and K. Haines (1999), Use of the temperature-salinity relation in a data assimilation context, *J. Phys. Oceanogr.*, *29*, 2011–2025.

Wang, O., I. Fukumori, T. Lee, and G. C. Johnson (2004), Eastern equatorial Pacific Ocean T-S variations with El Niño, *Geophys. Res. Lett.*, *31*, L04305, doi:10.1029/2003GL019087.

Zebiak, S. E., and M. A. Cane (1987), A model El Niño–Southern Oscillation, *Mon. Weather Rev.*, *115*, 2262–2278.

B. Cheng, I. Fukumori, T. Lee, and O. Wang, Jet Propulsion Laboratory, MS 300-323, 4800 Oak Grove Drive, Pasadena, CA 91109, USA. (bcheng@jpl.nasa.gov; if@pacific.jpl.nasa.gov; tlee@pacific.jpl.nasa.gov; owang@pacific.jpl.nasa.gov)